JOURNAL OF SPACECRAFT AND ROCKETS
Vol. 34, No. 2, March–April 1997

Hammerhead Wake Effects on Elastic Vehicle Dynamics

L. E. Ericsson*
Lockheed Missiles and Space Company, Inc., Mountain View, California 94040

An analysis has been performed of existing static and dynamic experimental results for hammerhead launch vehicles. The analysis shows that the always present flow phenomenon of hammerhead wake reattachment on the adjacent booster at high-subsonic speeds could generate aeroelastic instability powerful enough to endanger the structural integrity of the launch vehicle. The reason that this problem has not been discovered earlier is that it occurs only for a certain combination of vehicle geometry and elastic bending mode shape.

Nomenclature

c_A = aerodynamic damping
c_S = structural damping
c_{cr} = critical damping
D = maximum payload diameter
d = booster diameter
M = freestream Mach number
p = static pressure, coefficient $C_p = (p - p_\infty)/(\rho_\infty U_\infty^2/2)$
U = velocity
x = axial coordinate; Fig. 13
α = angle of attack
Δ = amplitude
θ_C = nose cone angle
θ_N = nose deflection angle
ξ = dimensionless axial coordinate, x/d
ϕ = mode deflection coordinate; Fig. 1

Subscript

∞ = freestream conditions

Introduction

CURRENT demands on unmanned launch capability have created renewed interest in large, nonrecoverable boosters. This, along with the advantage of using a well-tested, reliable bus for an arbitrary payload, has caused widespread use of launch vehicles with the hammerhead payload geometry used in the early 1960s. Recent analysis has revealed that, even after the latest update,[1] the NASA design criteria[2] do not consider a flow phenomenon unavoidably associated with hammerhead payloads, i.e., the hammerhead wake reattachment on the adjacent booster. It will be shown that this flow phenomenon could in some cases be a threat to vehicle structural integrity, even though the critical flight conditions are likely to be of short time duration. The highly nonlinear aerodynamics cause the destructive amplitude to be reached in a few cycles of oscillation.

Analysis

Although early results for a biconic-hammerhead geometry[3] (Fig. 1) showed the danger potential of the hammerhead-wake-reattachment flow phenomenon, for the particular mode shape tested, very modest negative aerodynamic damping was measured at $M = 0.95$ and 1.0. The large positive aerodynamic damping measured at $M = 0.9$, 0.6% of critical showed, however, that the wake reattachment on the 9.5-deg boattail generated large aeroelastic effects. In Fig. 2 flow sketches have been added to the results in Fig. 1 to illustrate the flow physics causing the different aeroelastic effects. At $M = 0.95$ and 1.0 the wake reattaches rather early on the windward side of the boattail, generating a negative normal force component. The generative process is very similar to that for the nose-induced flow separation on a blunt cone cylinder at a lower Mach number, $M = 0.9$, as illustrated by the results for the Saturn-Apollo booster with the escape rocket removed[4] (Fig. 3). The negative normal force generates a statically stabilizing moment at $M = 0.95$ and 1.0 in Fig. 2, which through accelerated-flow and time-lag effects[5] produces a dynamically destabilizing effect, resulting in the measured negative aerodynamic damping. At $M = 0.9$, however, the hammerhead wake does not reattach until downstream of the juncture between the boattail and the booster cylinder, judging by unsteady pressure measurements[6] (Fig. 4). Consequently, the negative normal force is in this case located aft of the forward nodal point in Fig. 2, generating a statically destabilizing/dynamically stabilizing moment,[5] resulting in the measured large positive damping.

If one considers the effect of a more realistic aft booster geometry, the mode shape in Fig. 2 could change as shown in Fig. 5, causing the nodal point to be located aft of the negative normal force, also at $M = 0.9$. If the apparent mass and frequency of the bending mode were to remain the same, the analysis in Ref. 5 predicts the aerodynamic damping to change as indicated by the solid data points in Fig. 5. That is, for this mode shape the aerodynamic damping at $M = 0.9$ would be roughly -1.0% of critical rather than $+0.6\%$. For liquid-propellant rockets the structural damping is usually only a fraction of 1%. The forward nodal point location could also be representative for the geometry shown in Fig. 5, but for the second mode rather than the first. These results illustrate the danger potential that is associated with the wake reattachment flow phenomenon on the 9.5-deg boattail. What happens in the case of a much steeper boattail, one that obeys the NASA design criteria,[2] such as the much tested configuration[7] shown in Fig. 6?

The experimental results[7] indicate that the wake reattachment on the downstream cylinder also generates a negative normal force. The large increase at $M = 0.895$ of the magnitude of this force indicates that the force generation could be of the discontinuous type associated with a sudden change of flow-separation topology, as in the case of a cone-cylinder geometry.[8] Figure 7 reveals that the hammerhead wake reattaches much farther downstream at $M = 1.0$ than at $M = 0.81$. Figure 8 shows the resulting difference in pressure distribution, in this case between $M = 0.88$ and 0.95. In Fig. 9 the results for $M = 0.895$ in Fig. 6 are shown by themselves to provide a direct comparison with the results in Fig. 8. From inviscid flow considerations one expects that the ambient flow conditions at the hammerhead shoulder, at the start of the boattail, would for the top side in Fig. 9 be comparable to those for $M = 0.95$ in Fig. 8, and those for the bottom side with those for $M = 0.88$ in Fig. 8. That is, the local ambient-flow Mach number at the hammerhead shoulder is higher on the top side in Fig. 9 than on the bottom side.

Thus, from inviscid flow considerations one would expect the reattachment pressures to be higher on the bottom side than on the top side in Fig. 9. Consequently, viscous flow processes are responsible for generating the change to the opposite type of reattachment pressures. Thus, the negative reattachment force generated by

Received Feb. 26, 1996; accepted for publication July 5, 1996.

*Retired; currently Engineering Consultant. Fellow AIAA.

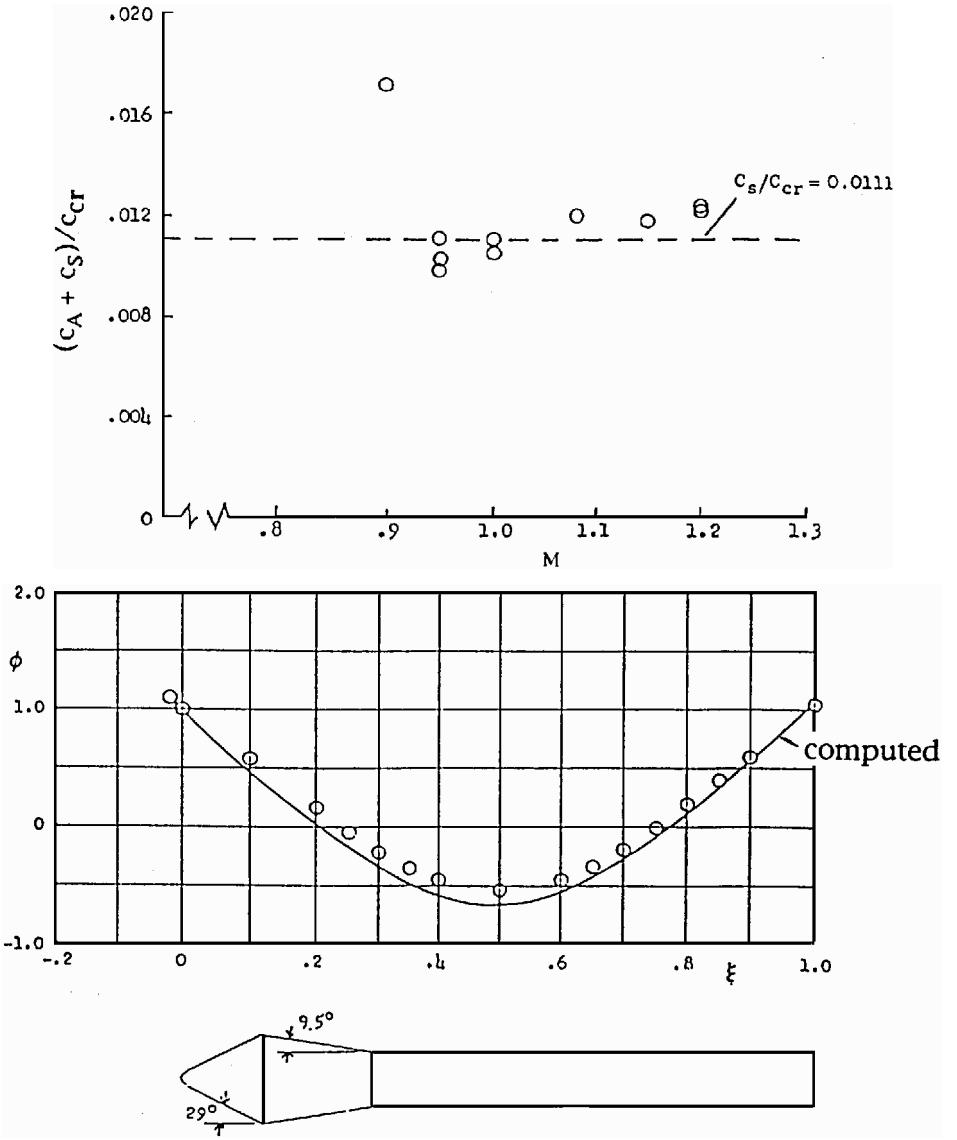

Fig. 1 Damping characteristics for the first bending mode of a biconic-hammerhead configuration.[3]

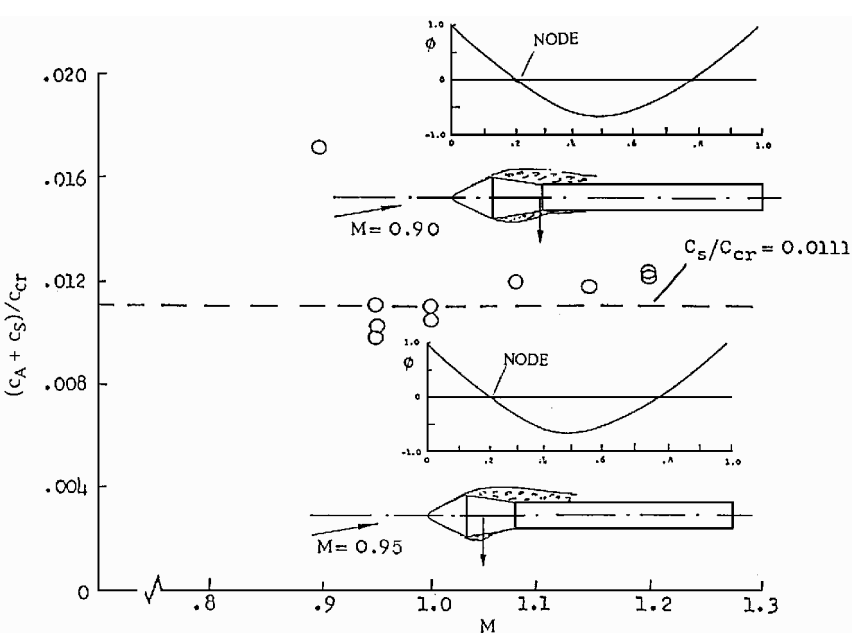

Fig. 2 Flow separation characteristics causing the different damping values at $M = 0.90$ and 0.95 in Fig. 1.

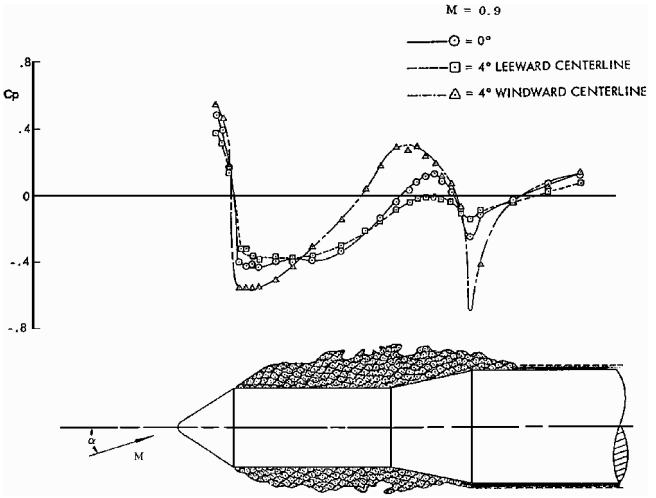

Fig. 3 Pressure distribution for nose-induced flow separation.[4]

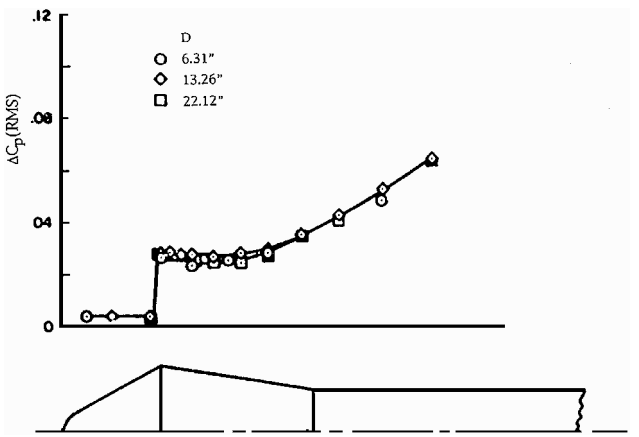

Fig. 4 Unsteady pressure distribution on biconic hammerhead geometry at $M = 0.90$ and $\alpha = 0$ (Ref. 6).

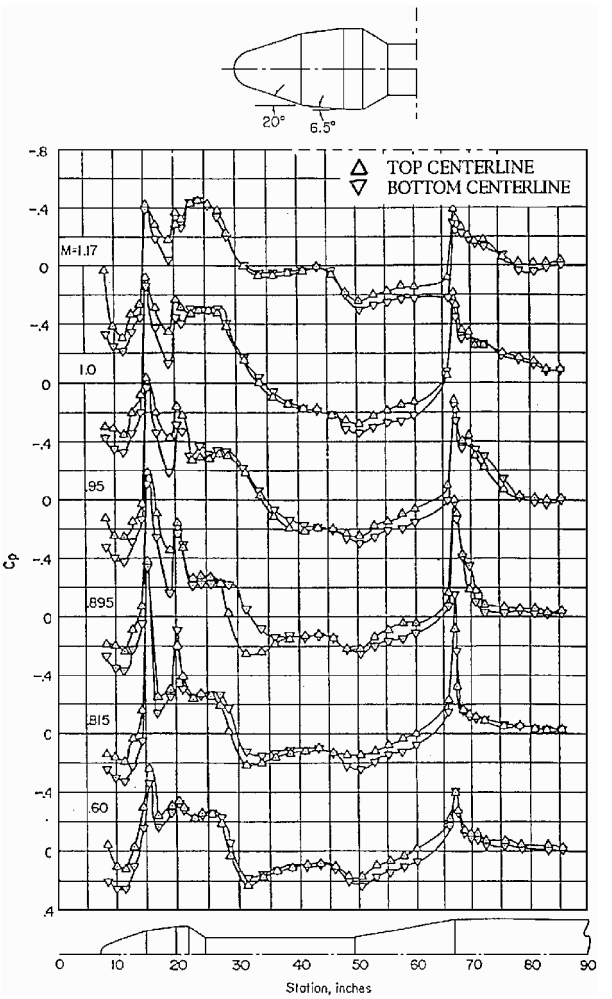

Fig. 6 Pressure distribution on a NASA-tested hammerhead geometry at $\alpha = 4$ deg for subsonic and transonic speeds.[7]

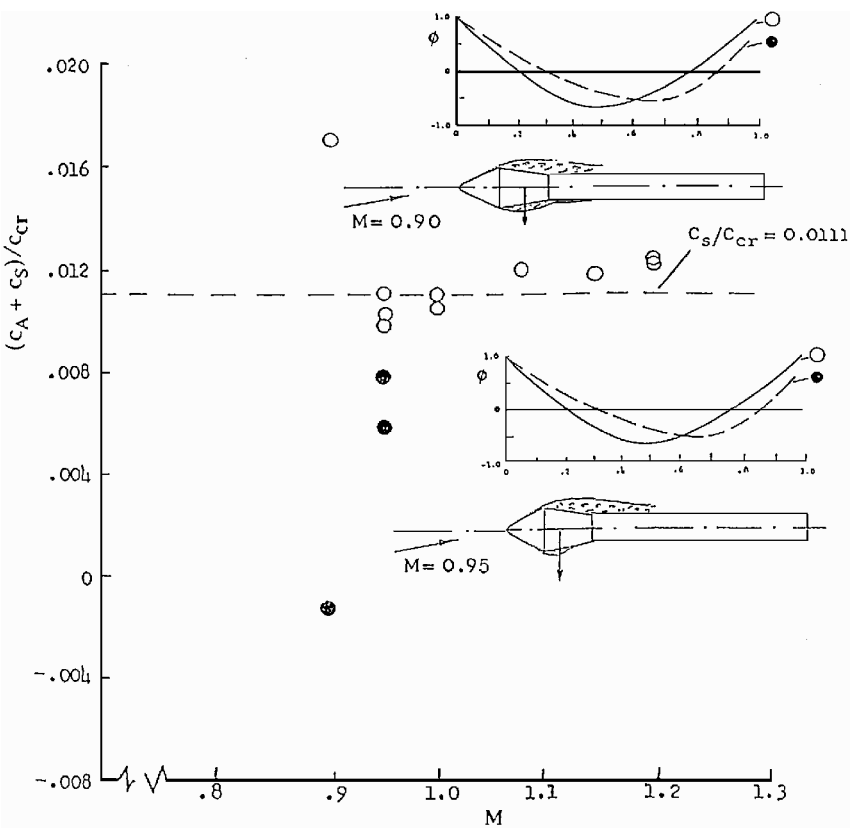

Fig. 5 Effects on damping of a slight change of mode shape for biconic hammerhead geometry.

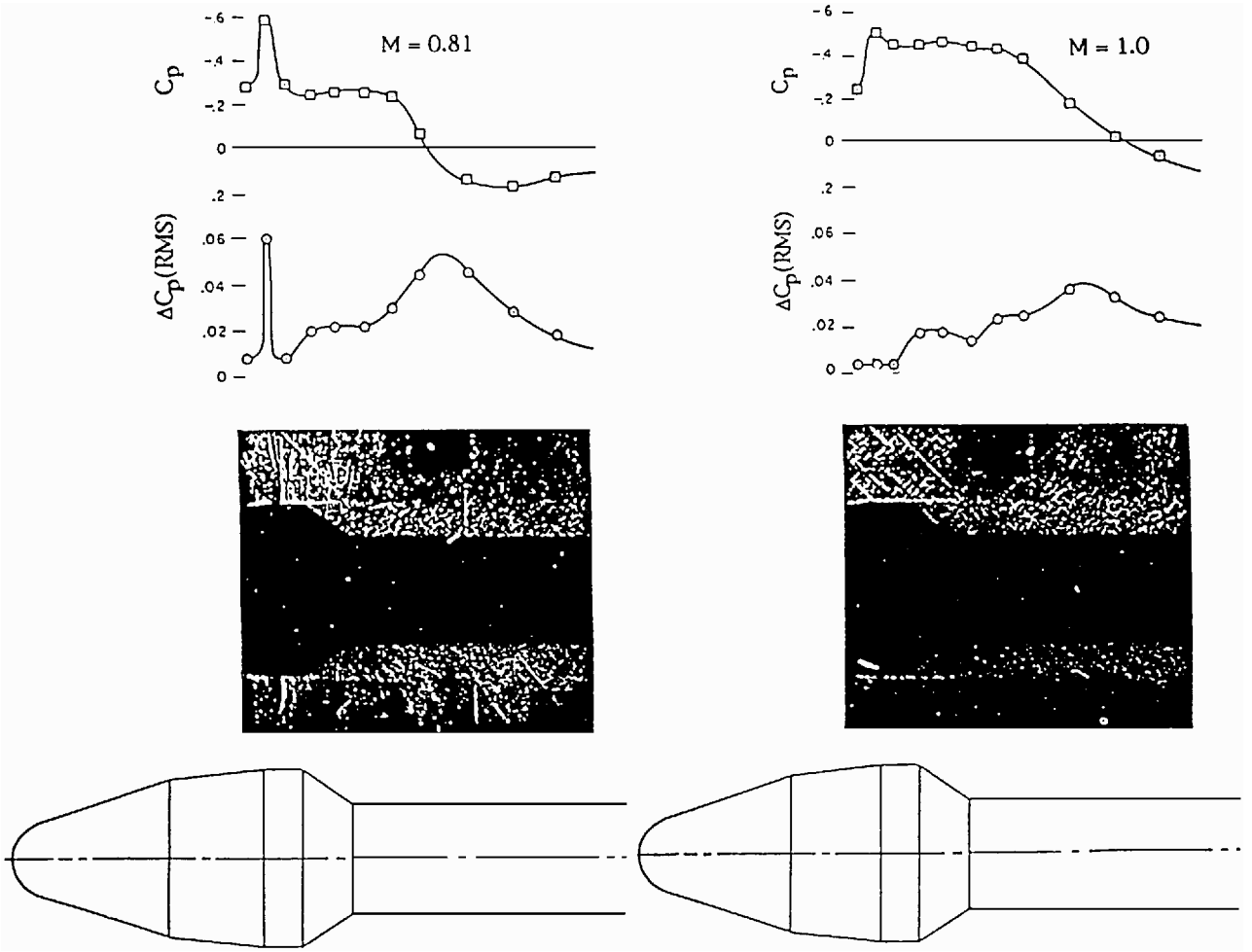

Fig. 7 Flow visualization results correlated with steady and unsteady pressure distributions on NASA-tested hammerhead geometry.[7]

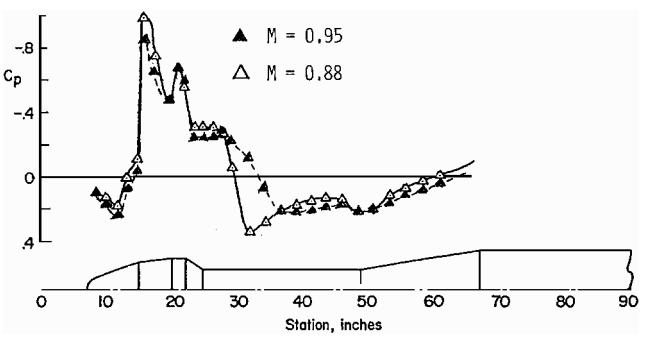

Fig. 8 Effect of Mach number on hammerhead pressure distribution at $\alpha = 0$ (Ref. 7).

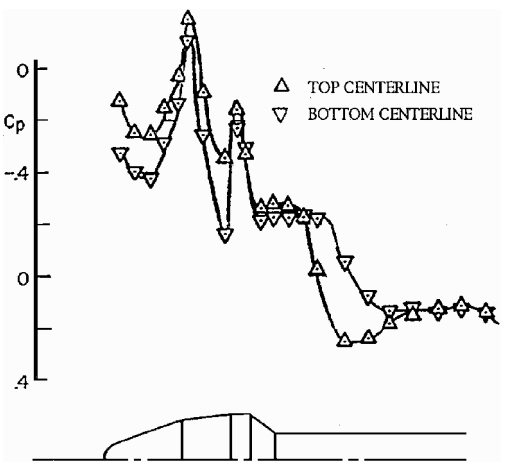

Fig. 9 Effect of 4-deg angle of attack on hammerhead pressure distribution at $M = 0.895$ (Ref. 6).

viscous flow processes is of larger magnitude than what is indicated by the experimental results in Fig. 9. To determine the true magnitude of the viscous contribution one needs to generate the inviscid pressures and associated loads. In the case of the cone-cylinder geometry,[8] the inviscid characteristics[9] were obtained using shock-expansion theory.[10] In the present case, Euler methods could provide the needed prediction capability.

The other hammerhead configuration in Ref. 7 gave the results shown in Fig. 10. Also in this case, as earlier in Fig. 6, large changes in the pressure distributions occur at high-subsonic speeds, e.g., at $M = 0.88$ and 0.95 in Fig. 10. However, comparing Figs. 6 and 10, one finds that the data trends are very different. For example, at $M = 0.88$ in Fig. 10 the negative normal force component is generated on the hammerhead cylinder, and the wake reattachment generates a positive force on the adjacent booster. What is causing this difference in separated flow characteristics?

In Fig. 11 the experimental results in Fig. 10 for $M = 0.88$ are shown in more detail to facilitate a comparison with those in Fig. 9 for $M = 0.895$. It was demonstrated in Ref. 1 that when the length of the hammerhead cylinder in Fig. 11 was reduced to 0.3 calibers, the pressure distribution shown in Fig. 12 resulted,[1] producing a statically stabilizing/dynamically destabilizing force, which caused the measured large buffeting loads.[11] Why, then, did the short cylinder in Fig. 9 not generate the load distribution shown in Fig. 12?

For the blunted 15-deg conical nose (Figs. 10–12) a sudden change of flow separation topology occurs, from retarded shock-

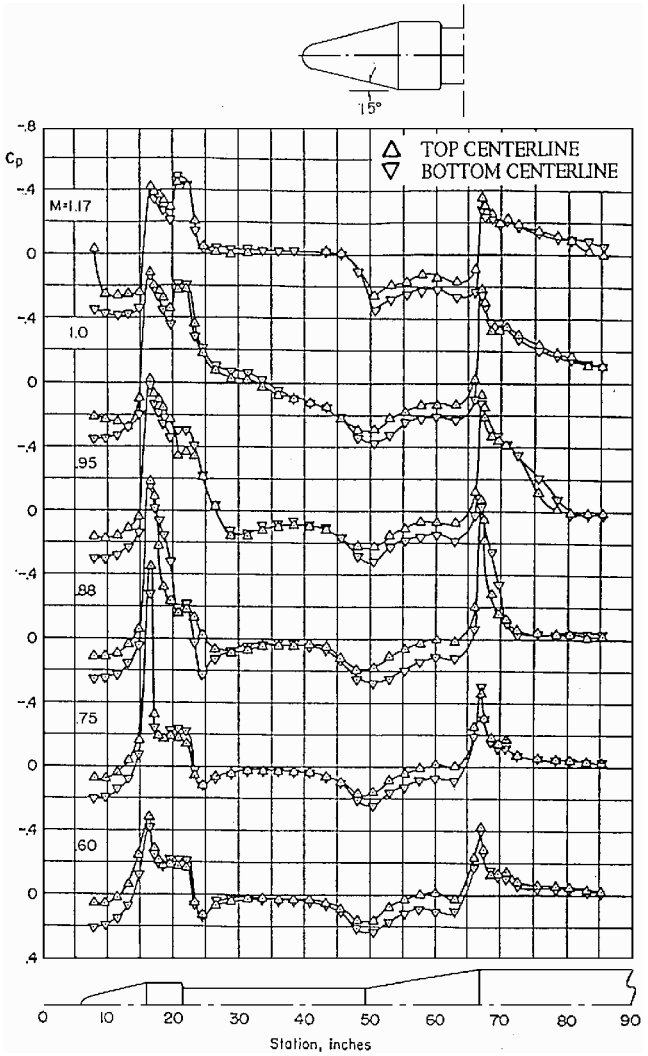

Fig. 10 Pressure distribution at α = 4 deg for subsonic and transonic speeds on a NASA-tested moderate hammerhead geometry.[7]

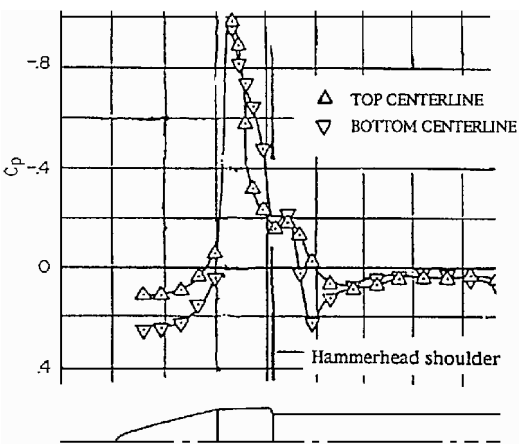

Fig. 11 Measured static pressure distribution on a hammerhead geometry at M = 0.88, α = 4 deg (Ref. 7).

induced separation[8,9] to the complete, nose-induced type observed on pointed cone cylinders[12,13] (Figs. 13 and 14). Figure 13 shows that at $M = 0.89$ the jump from retarded shock-induced to nose-induced flow separation occurs between $\alpha = 2$ and 4 deg for 20-deg cone angle and between 6 and 8 deg for 15-deg cone angle. Figure 14 shows the flow visualization results for the 20-deg cone cylinder. At $\alpha = 4$ deg the terminal normal shock does not penetrate to the surface on the top side. It is defused by the nose-induced

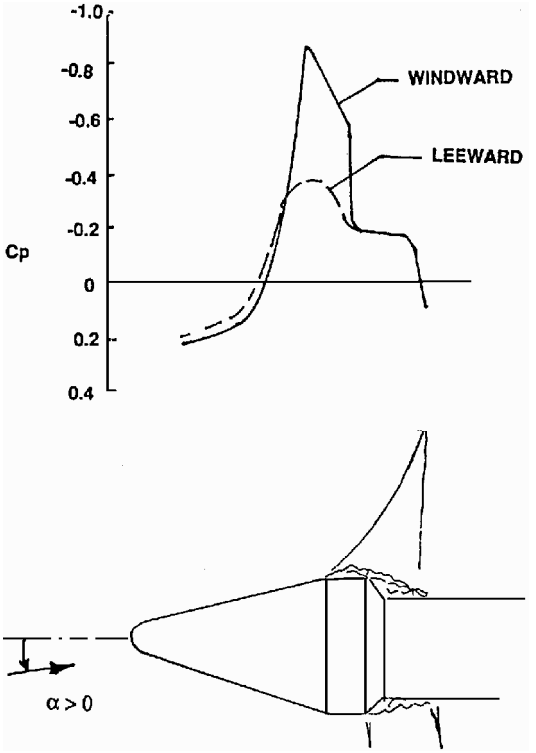

Fig. 12 Conceptual pressure distribution caused by sudden leeside flow separation at M = 0.89 on a 0.3-caliber hammerhead cylinder.[1]

flow separation. It is probable that the 33% nose bluntness on the 15-deg cone-cylinder configuration in Figs. 10–12 will cause the change of flow topology to occur earlier than for the sharp cone in Fig. 13, below $\alpha = 4$ deg, as indicated by the experimental results[7] in Fig. 10. So why does this not occur on the configuration in Figs. 6–9 also?

The cone-cylinder flow separation phenomenon received a great deal of attention in the 1960s because of its impact on launch vehicle aeroelastic stability.[8] It was found, really quite by accident, that by modifying the nose geometry, using a biconic rather than a conic geometry, the sudden change of flow separation topology was prevented from occurring[14] (Fig. 15). It can be seen that, due to the effect of the preseparation[8] at the biconic shoulder, the fresh boundary layer on the 12.5-deg conic frustum can negotiate the cone-cylinder shoulder without separating, up to $\alpha = 16$ deg. Thus, retarded shock-induced flow separation, similar to that for lower angles of attack, takes place. Changing the cone angles from 25–12.5 deg in Fig. 15 to 20–6.5 deg in Fig. 6 should, if anything, improve the efficiency of the biconic geometry to prevent nose-induced flow separation. Consequently, the hammerhead configuration in Fig. 6 should not experience nose-induced flow separation, in agreement with the experimental results.

Comparing the results for $M = 0.88$ in Fig. 10 with the results in Fig. 13 for cone-cylinder bodies, one can see that the change of flow separation topology in both cases generates a force couple, i.e., a negative normal force component followed by a positive one. The dynamically destabilizing effect will in this case be larger the closer the forward nodal point is to the force couple, as this will nullify much of the positive aerodynamic damping generated by the positive force component. Thus, in the case of the Saturn I–Block II launch vehicle[8] it was the second bending mode, not the first mode, that generated the largest aerodynamic undamping, approximately -1.0% of critical at $M = 0.9$ (Fig. 16). For the configuration in Fig. 10 the experimental results[7] indicate that at $M = 0.95$ only the forward negative load component was generated, and one would expect the first bending mode to experience the most adverse aeroelastic effect.

The test results in Fig. 16 were obtained through forced oscillations of an elastic model. In lieu of this very expensive and time-consuming test method, the partial mode simulation technique,

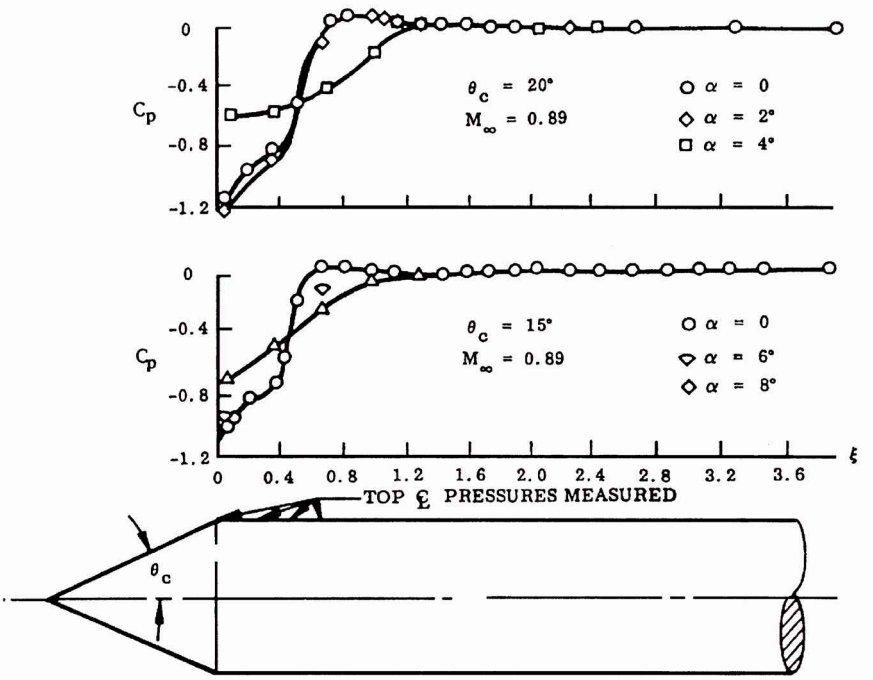

Fig. 13 Effect of cone angle on the occurrence of nose-induced flow separation on a cone cylinder.[13]

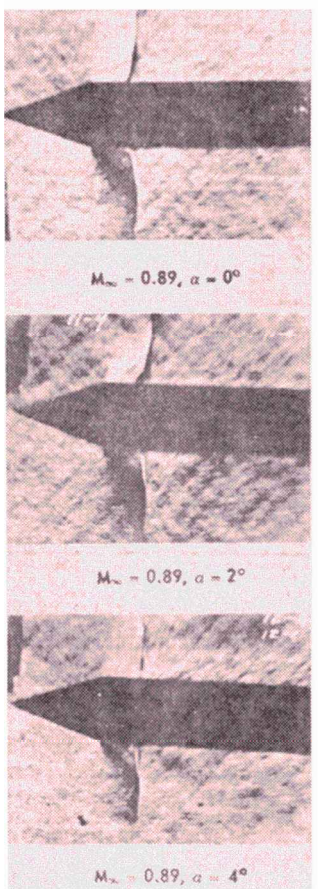

Fig. 14 Flow visualization of separated flow on a 20-deg cone cylinder at $M = 0.89$ and $\alpha = 0$, 2, and 4 deg (Ref. 13).

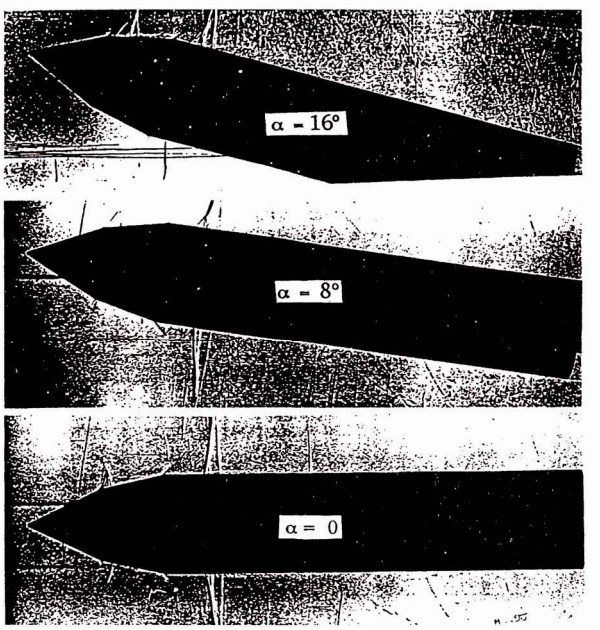

Fig. 15 Flow visualization of separated flow on 25–12.5 deg biconic-cone cylinder at $M = 0.9$ (Ref. 14).

described by Cole[15] and recently used by Cole and Henning,[11] will produce a conservative measure of the wake-induced undamping through the slightly exaggerated forward deflection. This substitution of the fully elastic testing method by essentially a rigid-body testing technique saves time and money.

Although no launch vehicle failure is known to have been caused by hammerhead wake reattachment effects, the analysis of existing experimental results presented here indicates that the potential for catastrophic aeroelastic response could often be present but overlooked. Because the aeroelastic consequences are so sensitive to configuration details, only a modest configuration change may be needed to avoid the problem altogether. Obviously, these hammerhead reattachment effects should be included in the NASA design criteria.[2]

The hammerhead payload geometry of the ill-fated Chinese Long March 2E launch vehicle[16] (Fig. 17) appears to have a geometry that could experience the sudden change of flow separation topology associated with a slender nose,[8] as well as the hammerhead wake reattachment phenomenon discussed here. Whether or not the reason that two launches ended in structural failure could be aeroelastic instability, caused by any of the two flow separation phenomena discussed here, can only be determined through an aeroelastic analysis of the type described in Refs. 5 and 8.

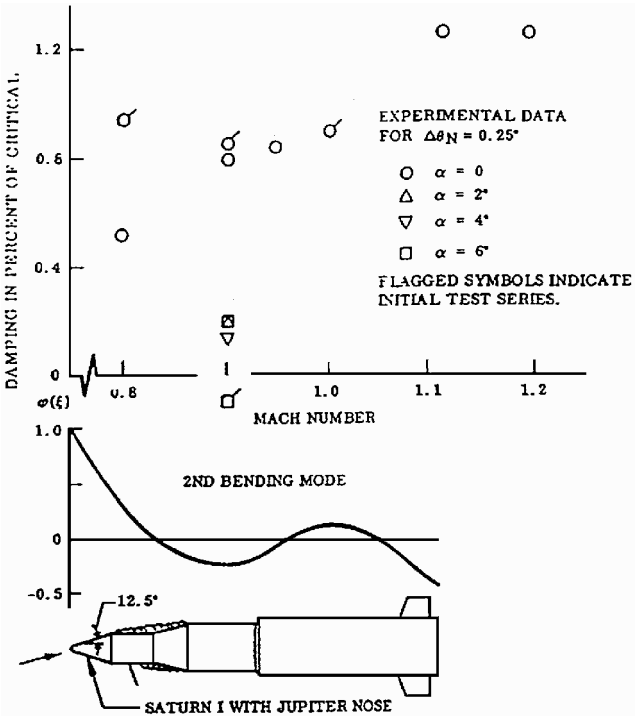

Fig. 16 Measured damping for the second bending mode of the Saturn I launch vehicle with Jupiter nose shroud.[8]

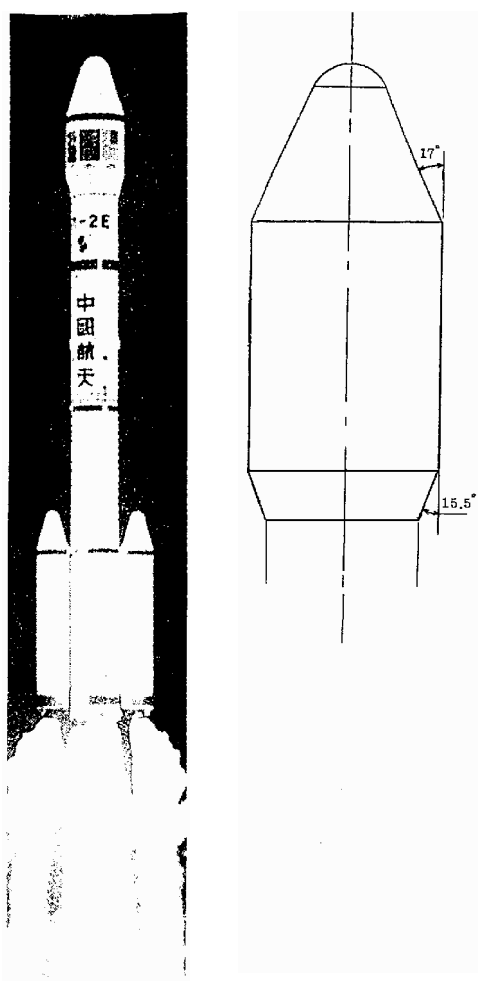

Fig. 17 Chinese Long March 2 E launch vehicle.[16]

Conclusions

A review of the existing database for hammerhead launch vehicles reveals that the reattachment of the hammerhead wake on the adjacent booster could be the source of aeroelastic instability for the lowest bending modes. This flow phenomenon is introduced when a shallow boattail is eliminated, following the established NASA design guidelines. The vehicle designer needs to be made aware of the associated potential danger.

When considering whether or not a launch vehicle could be subject to dynamic aeroelastic instability one should understand that all of the following conditions have to be satisfied.

1) The payload geometry has to be of the shape generating flow separation of the dangerous type.

2) One or more of the low-frequency bending modes has to have a mode shape that allows the flow separation to generate dynamic instability.

3) The Mach number/angle-of-attack time history must be such that the dangerous flow separation topology can be established.

If the aeroelastic analysis shows that dynamic instability could endanger the structural integrity of the launch vehicle, the only practical solution is to modify the payload geometry so that the dangerous flow separation topology cannot be established. Based on past experience, the required geometric change is usually minute.

References

[1]Reding, J. P., and Ericsson, L. E., "Hammerhead and Nose-Cylinder-Flare Aeroelastic Stability Revisited," *Journal of Spacecraft and Rockets*, Vol. 32, No. 1, 1995, pp. 55–59.

[2]Cole, S. R., and Henning, T. L., "NASA Space Vehicle Design Criteria, Vol. II: Structures, Part B; Launch and Exit, Section I; Buffeting," NASA SP-8001, May 1964, rev. Nov. 1970.

[3]Hanson, P. W., and Dogget, R. V., Jr., "Wind-Tunnel Measurements of Aerodynamic Damping Derivatives of a Launch Vehicle Vibrating in Free-Free Bending Modes at Mach Numbers from 0.70 to 2.87 and Comparisons with Theory," NASA TND-1391, Oct. 1962.

[4]Reding, J. P., and Ericsson, L. E., "Static Loads on the Saturn-Apollo Launch Vehicle," Lockheed Missiles and Space Co., Rept. LMSC/803185 (TM 53-40-143), Mountain View, CA, Aug. 1963.

[5]Ericsson, L. E., and Reding, J. P., "Fluid Dynamics of Unsteady Separated Flow. Part I-Bodies of Revolution," *Progress in Aerospace Sciences*, Vol. 23, 1986, pp. 1–84.

[6]Coe, C. F., "The Effect of Model Scale on Rigid-Body Unsteady Pressures Associated with Buffeting," *Symposium on Aeroelastic and Dynamic Modeling Technology* (AFFDL, Dayton, OH), Pt. 2, 1963, pp. 63–85 (RTD-TDR-63-4197).

[7]Coe, C. F., and Nute, J. B., "Steady and Fluctuating Pressures at Transonic Speeds on Hammerhead Launch Vehicles," NASA TM X-778, Aug. 1962.

[8]Ericsson, L. E., "Aeroelastic Instability Caused by Slender Payloads," *Journal of Spacecraft and Rockets*, Vol. 4, No. 1, 1967, pp. 65–73.

[9]Ericsson, L. E., "Loads Induced by Terminal-Shock-Boundary-Layer Interaction on Cone-Cylinder Bodies," *Journal of Spacecraft and Rockets*, Vol. 7, No. 9, 1970, pp. 1106–1112.

[10]Syvertson, C. A., and Dennis, D. H., "A Second-Order Shock-Expansion Method Applicable to Bodies of Revolution Near Zero Lift," NACA Rept. 1328, 1957.

[11]Cole, S. R., and Henning, T. L., "Dynamic Response of a Hammerhead Launch Vehicle Wind-Tunnel Model," *Journal of Spacecraft and Rockets*, Vol. 29, No. 3, 1992, pp. 379–385.

[12]Robertson, J. E., "Unsteady Pressure Phenomena for Basic Missile Shapes at Transonic Speeds," AIAA Paper 64-3, Jan. 1964.

[13]Robertson, J. E., and Chevalier, H. L., "Characteristics of Steady-State Pressures on the Cylindrical Portion of Cone-Cylinder Bodies at Transonic Speeds," Arnold Engineering Development Center, AEDC TDR-63-104, Aug. 1963.

[14]Ericsson, L. E., and French, N. J., "The Aeroelastic Characteristics of the Saturn IB SA-203 Launch Vehicle," NASA CR-76563, April 1966.

[15]Cole, H. A., Jr., "Dynamic Response of Hammerhead Launch Vehicles Buffeting," NASA TN D-1982, July 1963.

[16]Covault, C., "Asian Space Sector Poised for Explosive Growth," *Aviation Week and Space Technology*, July 2, 1995, pp. 25, 26.

R. M. Cummings
Associate Editor